Data-Driven Acoustic Communication Modeling for Undersea Collaborative Navigation

Douglas Horner and Geoffrey Xie
Naval Postgraduate School
Monterey, CA

Abstract—Feedback control of collaborative mobile systems requires assumptions with regards to wireless networking to bound system performance. Traditional assumptions include a physics-based signal propagation model which can be especially inaccurate in dynamic and cluttered communication environments. This paper addresses a data-driven approach for modeling signal strength. It presents local and global connectivity maps for providing greater resolution with respect to received signal strength over a bounded area. The approach may be particularly useful for enabling more flexible and robust multi-vehicle navigation.

Index Terms—Acoustic Communications, Collaborative Navigation, Kriging, Local Connectivity Map, Global Connectivity Map, Autonomous Underwater Vehicles.

1 Introduction

In the last ten years we've witnessed a marked improvement in unmanned mobile systems. Autonomous underwater, surface, aerial and ground vehicles are revolutionizing commerce, industry and the military. The vehicles permit a reduction in operating costs and an improvement in productivity for wide varieties of traditionally human-labor intensive activities. Their ability for wide-area sensor coverage, operations in harsh environments and persistence permits unprecedented monitoring and access. That said, there is general consensus that significant improvements are still possible.

One current trend is an emphasis on collaborative navigation for networked unmanned systems. It has the potential to impact a wide variety of operations through improvements in search rates, energy efficiency and system robustness. Key to collaboration is the wireless network. Better understanding with regard to the communications channel between vehicles directly impacts the ability to control the cooperative multi-vehicle system.

One can envision different approaches for communication channel estimation. On one extreme of the continuum is a pure physical modeling approach. It involves characterization of the communication channel through a predictive mathematical function. It accounts for the vagaries of the communication medium (air, water, space) and the nature of the signal (acoustic, radio, light) and the environmental impact to produce an estimate of the Received Signal Strength (RSS) between one vehicle attempting to communicate with another. It requires no statistical measurements of the channel.

On the other side of the continuum the estimation process is fully-determined by measurements. The benefit of this approach is that it requires no physical modeling. The model is built only from the measurements. This has particular utility in cluttered, dynamic areas where propagation of signals can result in unusual but effective communication paths. The weakness in the approach is that it is difficult to fully measure the environment with limited time, energy and resources.

This paper presents a data-driven technique for undersea acoustic communications channel estimation. It seeks a solution in-between the extremes of the continuum by building communications awareness with minimal sig-

U.S. Government work not protected by U.S. copyright

This is a DRAFT. As such it may not be cited in other works.
The citable Proceedings of the Conference will be published in
IEEE Xplore shortly after the conclusion of the conference.

nal measurements. The technique results in a Global Connectivity Map that, once built, permits mobile vehicles to estimate the probably of successfully communication with one or more of the other vehicles in the network throughout the survey region. This potentially results in a better distributed feedback control for multi-vehicle survey missions for several reasons.

First, it creates a more flexible system. Autonomous Underwater Vehicles (AUVs) can survey regions that are out of communications range, with the expectation that when necessary, they can navigate to a region where the probability of successful communications is high. Second, the GCM can be used as part of a criteria for determining how to partition a survey region such that the AUVs have a better capability for remaining fully-connected.

Third, the system will be more energy-efficient since better understanding of the communications landscape will result in faster and more accurate surveys. Fourth, this concept can be combined together with Simultaneous Localization and Mapping (SLAM) techniques that hold the promise to enable teams of AUVs to navigate accurately without surfacing for GPS fixes and without access to beaconing systems.

The data-driven approach is represented as a spatial optimal estimation problem. Kriging, a technique commonly used in the geostatistics community, is used for building a stochastic model of the RSS. The kriging process for acoustic connectivity maps has been described in an earlier paper [1]. At it's essence, it is an interpolation procedure that determines the mean and variance estimate by averaging surrounding measurements based on distance and a semi-variance relationship.

The paper proceeds as follows: Section II provides background and reviews related work. Section III defines the local and global connectivity maps and gives examples of each. Section IV presents two comparative examples of GCMs for providing initial insight into conducting efficient sampling. Section V presents conclusions. The results are based on acoustic modem datasets collected in Monterey Harbor, CA. Undersea acoustic communications was selected, in part, in recognition of the inherent difficulty associated with undersea wireless networking.

2 Background

Network Control Systems are defined by a distributed group of sensors and actuators with a closed control loop that is used to bound the system performance. The distributed coordination of multi-vehicle mobile systems is a subdiscipline of NCS where of critical interest is the impact of wireless communications on the feedback control loop.

A natural tool for modeling cooperative control and information flow within the mobile network is algebraic graph theory. Here the system is represented as a graph where the vertices are the mobile vehicles and the communication paths between the agents is represented as edges in the graph. A particularly useful framework within graph theory for determining conditions of stable cooperative control is the Laplacian matrix [2].

It is defined as $\mathbf{L} = \mathbf{D} - \mathbf{A}$ where $\mathbf{A}$ is the adjacency matrix for the vertices and the $\mathbf{D}$ matrix is the out-degree matrix where entries are limited to the diagonal and represent the number of outgoing network links of each vertex. It describes the state of connectedness of the network. A network is fully-connected when the Laplacian matrix is of full rank. Research into control of cooperative systems frequently involves the analysis of the controllability of the network using the Laplacian matrix.

Modeling of the graph edges can be defined stochastically whereby a probability is assigned to each edge that a transmission is successfully received from a source to a destination node. Of interest is the ability to accurately estimate the edges. This is useful for at least two reasons. First, it can be used to assess the probability that the network is fully-connected utilizing the Laplacian framework.

Second, each agent in the collaborative system typically runs a navigational filter. When the stability of an agent's filter is dependent on information obtained from a wireless network, the reliability of the communications channel becomes critically important to the stability of the filter. In fact, recent literature has established minimal probability bounds for Kalman filtering with intermittent observations [3].

With respect to past research, several communities have developed connectivity maps for radio-based networks. Larkin presented the idea of wireless signal strength topology maps in mobile adhoc networks [4]. The approach focuses on identification of areas with a particular signal loss [5].

Wireless localization is a field where the goal is to determine the location of a mobile device from wireless signals. Discussions of Ultrawide Bandwidth Signals and fundamental limits of ranging accuracy is given in [6] and [7]. A survey of indoor localization methodologies is given by Gholami [8].

In [9] and [10], Cottingham describes algorithms for processing large amounts of signal strength data for vehicle wireless coverage maps. Pogel and Wolf develop connectivity maps based on analysis of 3G network characteristics for vehicular traffic [11]. Additional research into radio frequency localization techniques include [12], [13], [14]. Recent surveys of underwater localization techniques are given in [15] and [16].

Kriging and Gaussian Process Models are two similar techniques that have been used for modeling wireless signal strength as a Gaussian random field. Ferris et al [17], use a Gaussian Process Latent Variable Model in combination with a novel WiFi-SLAM technique for building wireless signal strength maps. These are maps relative to a stationary WiFi access point.

Several authors have developed distributed kriging applications. Umer et al. presented a distributed kriging technique for estimating coverage holes in stationary wireless sensor networks [18], [19]. Cortes published a distributed Kalman Kriging filter for collaborative navigation [20]. In more recent research, Kim et al. present an interesting approach using Kriged Kalman filtering for cooperative cognitive radio sensing [21].

This paper includes three principal contributions. First a unifying framework for defining connectivity maps that is consistent with mobile cooperative multi-vehicle systems. Second, a significant collection of acoustic modem data in confined undersea operating areas. Third, the implementation of the framework for the stochastic RSS estimation using acoustic modem measurements.

3 Connectivity Maps

In this section, two types of connectivity maps are presented - a local and global connectivity map. The Local Connectivity Map (LCM) provides a signal estimate within a local reference frame. The Global Connectivity Map (GCM) provides an aggregate signal estimate referenced to a global coordinate framework. It is appropriate for survey operations in bounded regions.

4 Local Connectivity Map

The LCM is a random field (Z) within a bounded space in $\mathbb{R}^d$ (where normally d=2 or 3), where the stochastic variable of interest is a wireless signal strength. It is defined relative to the position and orientation of source node (the signal originator). The source node could be static or mobile.

An undersea example of a static application would be the optimal positioning of acoustic communication nodes with respect to system design objectives such as maximizing throughput. An example of a mobile application of a LCM would be a formation of AUVs, each with it's own LCM, where the goal of each is to simultaneously remain in formation and connected between immediate neighbors. These objectives are typically constrained by maximizing coverage or minimizing energy consumption.

Relative to the local reference frame, the goal is a stochastic estimate of the random field. For a Gaussian assumption this includes the mean and variance. The variance is useful since it can be used for prioritization of where to obtain measurements. Normally it is possible to make measurements at only a limited number of positions with respect to the local reference frame. Because of this it is necessary to ”fill in the gaps”. A technique called Communications Kriging is used to accomplish this.

Kriging is an Best Linear Unbiased Estimator (BLUE) interpolator. It provides an optimal estimate of a point of interest with respect to minimizing variance. A kriging technique generally consists of four steps: variogram analysis, solving a linear system of equations, and calculating the mean and variance. Key to the process is an estimate of a semi-variogram which measures the dissimilarity between measurements over an increasing lag distance. The technique used to build the LCM is known as ordinary kriging which includes a Lagrangian multiplier in the linear system of equations to ensure the solution vector sums to one.

Communication Kriging differs from traditional kriging in two ways. Kriging is commonly calculated with respect to a cartesian coordinate system using a euclidean distance metric for determining lag distances between observations. Since the LCM is measured relative to a source node it is necessary to convert euclidean distance relationships into range and bearings, since it is possible to have measurements strongly correlated but separated by significant distance.

Second, because a measurement of interest comes from a single source, it is possible to consider two semi-variograms. One that considers the range and another for radial relationships of measurements. The range semi-variogram uses measurements within a restricted bearing window to determine how measurements are dissimilar with respect to range.

The radial semi-variogram uses measurements within a minimum and maximum radial distance from the source node to determine how measurements are dissimilar with respect to bearing. The radial semi-variogram is useful for potentially providing a better estimate, where if the semi-variance relation is nearly constant it signifies that the random field is isotropic and additional measurements can be used to improve the overall estimate.

In summary, the range semi-variogram provides a measure of dissimilarity between observations at different ranges from the source node while the radial semi-variogram provides a measure of dissimilarity with respect to observations at different bearings from the source node.

The kriging estimate calculates a mean and variance. The two semi-variograms can be used to calculate two estimates of the random field at a point of interest. This can be stochastically averaged by weighting each measurement by the opposing variance.

The strength of the Communications Kriging approach is that it takes into account the source-based nature of the signal. This provides a unique capability for modeling anisotropic environments that are typical in difficult communication environments. The downside is that the stochastic average has a tendency for producing overly conservative variance estimates.

4.1 Example LCM

In July 2012, undersea acoustic modem datasets were collected in Monterey Bay, Monterey CA. Over the course of a single day, a Woods Hole Oceanographic Institution (WHOI) gateway buoy was placed a five different sites within the harbor. It had a 27kHz micro-modem deployed at 4 meters depth. The destination node of the acoustic transmissions was a micro-modem transducer mounted from a small surface craft that transited the bay at slow speeds (3 knots). Transmissions from the source node occurred every 10 seconds. Transmissions between the source and destination was a standard mini-packet that included signal statistics such as RSS, Signal to Noise Ratios (SNR) and Noise levels.

Figure 1 shows an overhead image of Monterey Harbor with 1851 RSS measurements relative to the S_1 source node. The position measurements are color-coded, reflecting the measurement range (1-30 dB).

Figure 2 shows the resulting empirical range semi-variogram used for determining the semi-variance relation between points that differ by a range lag-distance. Figure 3 plots the empirical radial semi-variogram for several ring ranges. The linear plot and low semi-variance of the radial semi-variogram at shorter ranges (0-50m, 50-100m and 100-150m) implies that the measurements are isotropic.

The kriging mean estimate is given in figure 4. The kriging variance is not shown. The map

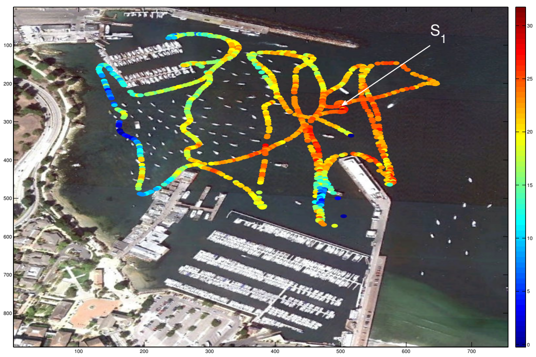

Fig. 1. An overhead image of Monterey Harbor with 1851 RSS measurements that are a result of acoustic undersea communication between a source node S_1 and a destination node.

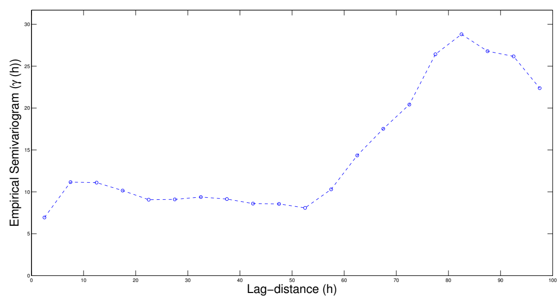

Fig. 2. The range semi-variogram from RSS measurements in a bearing window from 135 to 180 degrees with respect to the source node

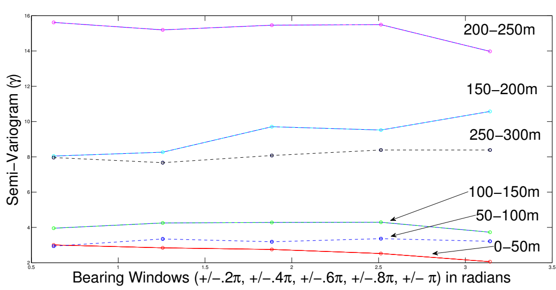

Fig. 3. The radial semi-variogram from RSS measurements at several radial ranges.

resolution for both is $10m^2$. Notice the environment has induced an anisotropic random field and the process has likely produced a better estimate than possible through physical modeling.

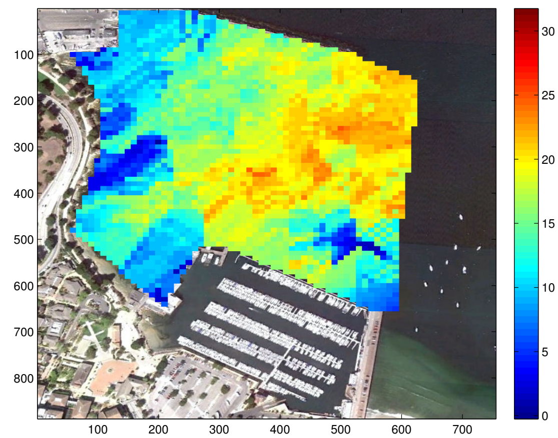

Fig. 4. The overlay is the LCM mean estimate of the RSS. Map resolution is 10 meters squared.

4.2 LCM Accuracy

LCM accuracy is impacted through three main sources of errors: Sensor-related, location estimation and modeling. Sensor-related measurement errors reflect the ability of the WHOI μ-modem to measure the ambient noise in the environment and the RSS. The RSS is considered the more reliable of the two measurements since it is measured over the entire length of the incoming packet. Conversely the noise measurement is made over a small window due to the modem constraints of real-time operations.

In assessing the quality of the LCM, it is necessary to consider issues of prediction accuracy and optimal sampling strategies. Prediction accuracy is the ability of kriging techniques to accurately interpolate data to provide minimal errors at locations where there are no direct measurements. Optimal sampling strategies reflect competing objectives of minimizing the number of samples while ensuring that the LCM error is reduced to an acceptable level. These strategies reflect the goal of creating an LCM while not wasting valuable resources such as time and energy.

One common way to determine errors in ordinary kriging models is the variance of the difference between the estimated value $\hat{Z}(\mathbf{x}^*)$ and the measurement $Z(\mathbf{x})$. This known as the kriging error. A common methodology for determining the kriging error is K-fold cross-

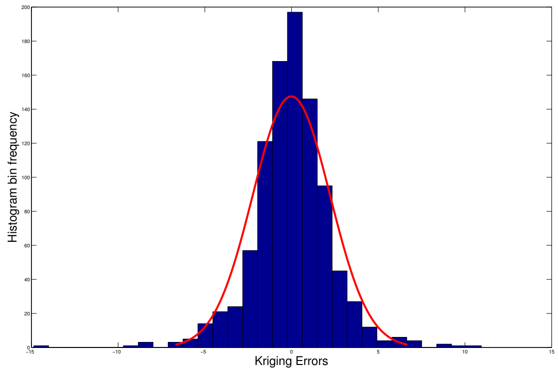

Fig. 5. The histogram plot gives the frequency of kriging errors associated with the S_1 acoustic modem dataset collected in Monterey Harbor, CA in July 2012. A best fitting Gaussian distribution is superimposed in red $\mathcal{N}(-.002, 2.2891)$

validation. It divides the data into k equal-sized partitions and for each iteration of the process one of the partitions is removed and the model is built with the remaining data and validated with the removed partition.

This process is repeated and each time a different partition is removed and subsequently used for validation. The validation process takes each of the withheld data points and compares them to the closest prediction point in the model. The difference between the prediction and the data is the kriging error ($\epsilon_{ke} = \hat{Z}(\mathbf{x}_0) - Z_{nn}(\mathbf{x})$), where $Z_{nn}(\mathbf{x})$ is the nearest neighbor to the withheld validation point $\hat{Z}(\mathbf{x}_0)$.

Given a theoretical variogram, the kriging error should have a zero mean $E[\epsilon_{ke}] = 0$ and Gaussian distribution with variance σ_K^2. This can be graphically checked by looking at the kriging error histogram of the aggregated k-fold results. Figure 5 shows histogram for for the S_1 dataset with a Gaussian distribution overlaid in red (parameters). As can be seen by the graphic, the histogram of the kriging errors generally conforms to the expectation of an accurate model.

5 Global Connectivity Map

The LCM is relative to the pose of the source node. With a system of collaborative vehicles, the emphasis is on the ability to estimate signal strength relative to any two points within a survey space. This is not possible with a single LCM. What is necessary is a connectivity map that is not relative to the position of the communicating agents in the network. That is now addressed.

The Global Connectivity Map (GCM) is a natural extension of the LCM. It is referenced to global coordinates rather than the body coordinates of a vehicle. The utility of the GCM is in the ability to estimate RSS between any locations in the bounded survey region.

The GCM can be a useful tool for improving multi-vehicle collaborative navigation by providing a better model for determining the probability of successful communications. This, in turn, can be used for positioning vehicles to ensure that the probability of successful communications remains at a level that ensures the multi-vehicle feedback system remains stable.

The impact of an accurate GCM can improve system robustness, flexibility and effectiveness. Some examples include:

1) An agent can temporarily move out of communication range with the knowledge of where to return for a high probability of connecting back into the network.
2) An area can be partitioned, taking into consideration the communication landscape such that it optimizes the probability that networked agents remain fully-connected.
3) Development of trajectories within the system such that area coverage constraints are obeyed.

The GCM is defined as a bounded survey space Ω in $\mathbb{R}^d$ that is partitioned into a spatial tessellation ($\Omega = \cup_{i,j=1}^{n,m} \Omega_{nm}$) and relative to the defined center tile cell $\Omega_{nm}(\mathbf{x_c})$ we seek to predict the mean and variance of the random field $Z_{nm}(\mathbf{x}), \forall \mathbf{x} \in \mathbb{R}$ (equivalently an LCM) out to a maximum distance R_{max}. Each cell in the tessellation has

- An LCM that models RSS relative to a central node.
- A course, scalar estimate of the overall ability to communicate omni-directionally.
- A course, scalar estimate of the overall uncertainty in the region.
- A discrete number of vectors where by each corresponds to a bearing (relative to

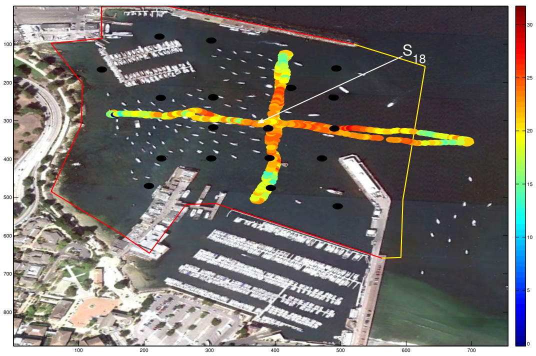

Fig. 6. The overhead image includes an overlay of the GCM central nodes (in black) and provides the measurements of a single data set relative to the central source node S_{18}. A total of 727 RSS measurements were collected for S_{18}.

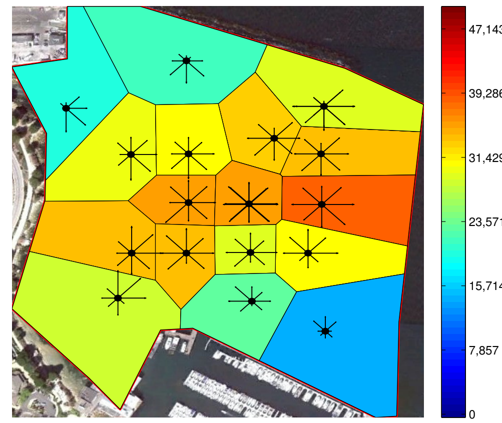

Fig. 7. The GCM created from the March 2013 data collection. The colors correspond to general assessments of signal strength and the vectors emanating from the sources nodes correspond to directional signal strength.

the LCM center) and each element in the vector corresponds to a mean and variance estimate at a particular distance from the center node.

The scalar estimates of communication effectiveness and uncertainty can be defined over a continuous space as integrals over polar coordinates, where the integrating function is the equation for the kriging mean and (separately) the kriging variance. In a discrete implementation, a Riemann sum is used.

Note that the vectors associated with each tile provides a simplified, graphic depiction of the anisotropic behavior of the random field by providing an estimate of the strength of the signal with respect to bearing. Greater vector magnitude corresponds to better RSS values over a greater distance.

5.1 Example GCM

In Monterey Harbor, March 2013, acoustic modem RSS measurements were again collected. Over the course of two days, the static acoustic communications buoy was positioned at 17 different locations, three sites were surveyed twice for a total of 20 datasets. A total of 7348 measurements were taken. Figure 6 shows the positions of the static buoys and gives an example of a single data collection relative to one of the static nodes.

Figure 7 shows the resulting GCM map. It is based on a Voronoi spatial tessellation. Each of the cells of the GCM has an estimate of the RSS out to a maximum distance of 300m or the intersection with the bounded search space. As described above, this is summarized using the Riemann sum to provide a course estimate of communication effectiveness and uncertainty. The figure includes directional estimates of signal strength. They emanate from the control point of the tessellation cell.

Both the color mapping and the directional estimates of signal strength are calculated with respect to a reference (or maximal) value. The value was determine from an ideal measurement environment obtained from acoustic observations in the open ocean.

Note that the best areas for communication generally coincide with center of the harbor channel and the deepest most open regions of the harbor. This might be expected. A possibly unanticipated result is the poor RSS in the southeastern portion harbor. In fact it was, by far, the worst area for acoustic communications. Somewhat unexpectedly, the communication was good in the harbor's southwestern shallow water. Overall the GCM seems to nicely summarize the aggregate ability to communicate.

6 GCM Measurement Strategies

A natural question with respect to building the GCM is to determine the optimal sampling strategy of spatial measurements that balances time and energy with accuracy. A good strategy would determine trajectories for multiple vehicles that permits measurements in locations to simultaneously build the multiple random fields comprising the GCM.

There are two fundamental aspects of the GCM. The first is the anisotropic nature of the random field. This has already been introduced and is the uniformity of the RSS estimate with respect to the bearing from the source node. The second is the homogeneity within the Voronoi cell. The GCM makes a simplifying assumption that all estimates within the cell boundary are the same as the estimate with respect to the defined central node of the random field. This is the map resolution of the GCM.

When this assumption is valid the cell is homogeneous. The source node could be located anyway within the cell boundary and the resulting random field would be the same. The converse is an example of a non-uniform or nonhomogeneous GCM cell. The movement of the central node to other positions within the LCM boundary would result in significantly different estimate. In this case, the cell boundaries are poorly defined but were made necessary, possibly, due to the limited number of available measurements.

Table 1 summarizes these general characteristics. Each entry reflects an efficient strategy for accurately building the GCM in a given environment. The top left entry is a GCM that is characterized by a relatively homogeneous, isotropic field. This is an ideal situation where it is possible to estimate the GCM with minimal measurements and the GCM cells are characterized by a larger area. The bottom right entry is the opposite situation, a difficult communications environment that is characterized by an nonhomogeneous and anisotropic environment that requires denser measurements with a GCM cell resolution that must be smaller in order to create an accurate map.

The off-diagonal entries represent intermediate situations. The top right is an environment with an nonhomogeneous, isotropic field which requires a sparser number of measurements and smaller GCM cells. The top left environment is characterized by a homogeneous, anisotropic field which requires denser measurements and supports larger GCM cells.

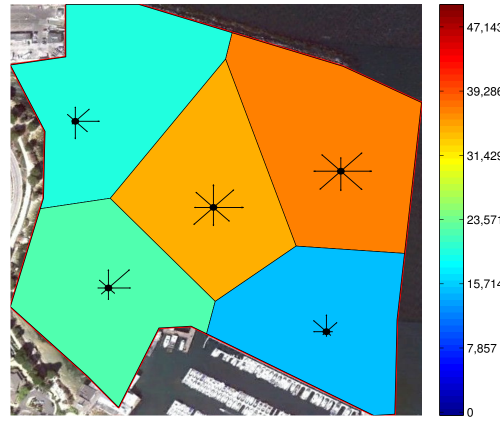

Fig. 8. The GCM created from the July 2012 data collection. The colors correspond to general assessments of signal strength and the vectors centered on the central cell node correspond to directional signal strength.

The data sets collected in July 2012 and March 2013 reflect these off-diagonal table entries. In July 2012, only a few (5) fixed acoustic buoy locations were selected but the spatial measurements more completely covered the bounded survey region. This corresponds to the bottom left entry in the table and would be an appropriate data collection strategy for a homogeneous, anisotropic GCM. In March 2013, there were a significantly greater number of acoustic buoy locations (20) but each survey consisted of a more limited number measurements. This strategy corresponds to the top right entry of the table, one that is appropriate for an inhomogeneous, isotropic environment.

The GCM resulting from the July 2012 datasets is given in figure 8. It has a larger map resolution but notice that the overall ability to communicate generally conforms to the GCM in figure 7.

TABLE 1
GCM Data Collection Strategies

	Homogeneous	Non-homogeneous
Isotropic	Sparse measurements Larger GCM map resolution	Sparse measurements Smaller GCM map resolution
Anisotropic	Dense measurements Larger GCM map resolution	Dense measurements Smaller GCM map resolution

7 Conclusion

The paper presented a methodology for Received Signal Strength (RSS) estimation between mobile collaborative agents. It is based on local and global connectivity maps. The Local Connectivity Map (LCM) provides an RSS estimate relative to the pose of a source node. The Global Connectivity Map (GCM) provides a RSS estimate relative to a global coordinate system. It is based on constructing a tessellation of LCMs on a bounded survey region.

Both rely on communication kriging techniques for spatial estimation of a gaussian random field. The methodology potentially provides a better stochastic estimate for the probability of successful communications that can be used to ensure stable system control of a group of collaborating mobile unmanned systems.

Future research will include the following: Calculating the probability of successful communication based on the RSS, developing collaborative navigation strategies for the quick and accurate building of the GCM and incorporating temporal considerations into the methodology.

Acknowledgment

This research was made possible through the Office of Naval Research (ONR) N0001413AF00002. The authors would like to thank Dr. Tom Swean from ONR and the NPS Center for Autonomous Vehicle Research.

References

[1] D. Horner and G. Xie, "Undersea acoustic communication maps for collaborative navigation," in *Autonomous Underwater Vehicles (AUV), 2012 IEEE/OES*. IEEE, 2012, pp. 1–7.

[2] J. Fax and R. Murray, "Graph laplacians and stabilization of vehicle formations," 2001.

[3] S. Kar and J. M. Moura, "Moderate deviations of a random riccati equation," *Automatic Control, IEEE Transactions on*, vol. 57, no. 9, pp. 2250–2265, 2012.

[4] H. Larkin, "Wireless signal strength topology maps in mobile adhoc networks, embedded and ubiquitous computing," in *International Conference EUC2004*, pp. 538–547.

[5] ——, "Wireless signal strength topology maps in mobile adhoc networks," *Embedded and Ubiquitous Computing*, pp. 85–100, 2004.

[6] D. Dardari, A. Conti, U. Ferner, A. Giorgetti, and M. Win, "Ranging with ultrawide bandwidth signals in multipath environments," *Proceedings of the IEEE*, vol. 97, no. 2, pp. 404–426, 2009.

[7] Y. Shen and M. Win, "Fundamental limits of wideband localizationpart i: a general framework," *Information Theory, IEEE Transactions on*, vol. 56, no. 10, pp. 4956–4980, 2010.

[8] M. Gholami, "Positioning algorithms for wireless sensor networks," 2011.

[9] D. Cottingham, R. Harle, and A. Hopper, "Constructing accurate, space-efficient, wireless coverage maps for vehicular contexts," in *Proceedings of the 4th Annual International Conference on Wireless Internet*. ICST (Institute for Computer Sciences, Social-Informatics and Telecommunications Engineering), 2008, p. 44.

[10] D. Cottingham, "Vehicular wireless communication," *Computer Laboratory, University of Cambridge*, 2009.

[11] T. Pogel and L. Wolf, "Analysis of operational 3g network characteristics for adaptive vehicular connectivity maps," in *Wireless Communications and Networking Conference Workshops (WCNCW), 2012 IEEE*. IEEE, 2012, pp. 355–359.

[12] J. Biswas and M. Veloso, "Wifi localization and navigation for autonomous indoor mobile robots," in *Robotics and Automation (ICRA), 2010 IEEE International Conference on*. IEEE, 2010, pp. 4379–4384.

[13] K. Yedavalli and B. Krishnamachari, "Sequence-based localization in wireless sensor networks," *Mobile Computing, IEEE Transactions on*, vol. 7, no. 1, pp. 81–94, 2008.

[14] A. Bo, Z. Zhang-dui, Z. Gang, and L. Jian-ping, "Novel statistical processing methods for wireless field strength prediction," *Consumer Electronics, IEEE Transactions on*, vol. 55, no. 4, pp. 1805–1809, 2009.

[15] M. Erol-Kantarci, H. Mouftah, and S. Oktug, "A survey of architectures and localization techniques for underwater acoustic sensor networks," *Communications Surveys & Tutorials, IEEE*, vol. 13, no. 3, pp. 487–502, 2011.

[16] G. Han, J. Jiang, L. Shu, Y. Xu, and F. Wang, "Localization algorithms of underwater wireless sensor networks: A survey," *Sensors*, vol. 12, no. 2, pp. 2026–2061, 2012.

[17] B. Ferris, D. Hähnel, and D. Fox, "Gaussian processes for signal strength-based location estimation," in *In Proc. of Robotics Science and Systems*. Citeseer, 2006.

[18] M. Umer, L. Kulik, and E. Tanin, "Kriging for localized

spatial interpolation in sensor networks," in *Scientific and Statistical Database Management*. Springer, 2008, pp. 525–532.

[19] ——, "Spatial interpolation in wireless sensor networks: localized algorithms for variogram modeling and kriging," *Geoinformatica*, vol. 14, no. 1, pp. 101–134, 2010.

[20] J. Cortés, "Distributed kriged kalman filter for spatial estimation," *Automatic Control, IEEE Transactions on*, vol. 54, no. 12, pp. 2816–2827, 2009.

[21] S.-J. Kim, E. Dall'Anese, and G. B. Giannakis, "Cooperative spectrum sensing for cognitive radios using kriged kalman filtering," *Selected Topics in Signal Processing, IEEE Journal of*, vol. 5, no. 1, pp. 24–36, 2011.